

Received January 27, 2020, accepted February 9, 2020, date of publication February 12, 2020, date of current version February 20, 2020.

Digital Object Identifier 10.1109/ACCESS.2020.2973399

# Development of a Wideband 220-GHz Subharmonic Mixer Based on GaAs Monolithic Integration Technology

YILIN YANG<sup>1</sup>, BO ZHANG<sup>1</sup>, (Senior Member, IEEE), DONGFENG JI<sup>1</sup>,  
XIANGYANG ZHAO<sup>2</sup>, YONG FAN<sup>1</sup>, AND XIAODONG CHEN<sup>3</sup>, (Fellow, IEEE)

<sup>1</sup>School of Electric Science and Engineering, University of Electronic Science and Technology of China, Chengdu 611731, China

<sup>2</sup>National Key Laboratory of Application Specific Integrated Circuit, Hebei Semiconductor Research Institute, Shijiazhuang 050000, China

<sup>3</sup>School of EECS, Queen Mary University of London, London E1 4NS, U.K.

Corresponding author: Bo Zhang (zhangbouestc@yeah.net)

This work was supported by the National Natural Science Foundation of China (NSFC) under Grant 91738102 and Grant 61771116.

**ABSTRACT** A wideband 220 GHz subharmonic mixer based on monolithic integration technology is proposed in this paper. It features 12  $\mu\text{m}$ -thick GaAs membrane with anti-parallel Schottky diodes working at THz band monolithically integrated on the membrane. The optimization principles of low-parasitics Schottky diodes and the fabrication process of GaAs MMIC membrane diodes are elaborated. To realize optimum performances of the mixer, the dimensions of the integrated diodes and the matching network are optimized with harmonic balance simulation and load-pull techniques. An IF low pass filter with compact microstrip resonance cell (CMRC) configuration and an improved perpendicular coax-to-microstrip connection are used to realize wide IF band. The measured results show that the single sideband (SSB) conversion loss of this mixer is less than 10.5 dB from 185 to 255 GHz with fixed IF of 1 GHz, while the double sideband (DSB) noise temperature is better than 1400 K in this frequency range. Using fixed local oscillator (LO) frequency of 110 GHz, the measured SSB conversion loss is 7.4–10.7 dB within 185–255 GHz, indicating the good performances of the mixer with IF from DC to 35 GHz. The GaAs monolithic integration technology provides an approach for massive manufacturing of identical circuits and the proposed mixer with wideband characteristics will be applied in 220 GHz imaging systems in the near future.

**INDEX TERMS** Wideband, subharmonic mixer, submillimeter wave, monolithic microwave integrated circuit (MMIC), Schottky diode.

## I. INTRODUCTION

In the last two decades, submillimeter wave and THz band have drawn interest for a wide range of applications such as communication, imaging, astrophysics, bio-medicine and so on along with the electrical devices and component at higher frequency. Among others, submillimeter and THz wave imaging exhibit benefits over either lower or higher frequency band. For example, huge absolute bandwidth can improve the resolution of the radar system; short wavelength at this frequency band enable small diameter yet high gain antenna; the characteristics of submillimeter and THz wave provide the possibility of obtaining images under extreme situations,

The associate editor coordinating the review of this manuscript and approving it for publication was Yuhao Liu.

such as low visibility scenarios provoked by clouds, fog, rain or even dust storms.

In these years, a number of active or passive imaging systems have been reported at submillimeter wave and THz band [1]–[4]. Among these systems, imaging arrays are applied to realize high isolation and real time imaging [5]–[8]. For solid-state THz band imaging systems, the heterodyne receivers based on wideband mixers are most commonly used. In active imaging systems, the mixers work with fixed IF frequencies while the RF bandwidths decide the resolution of the system. For passive imaging systems, the receivers are performed with fixed LO frequencies, and the RF bandwidths are also influenced by the IF bandwidth. Therefore, wide IF band is also required for these mixers.

The basic configuration of the receiving front-end in UESTC (University of Electronic Science and Technology of

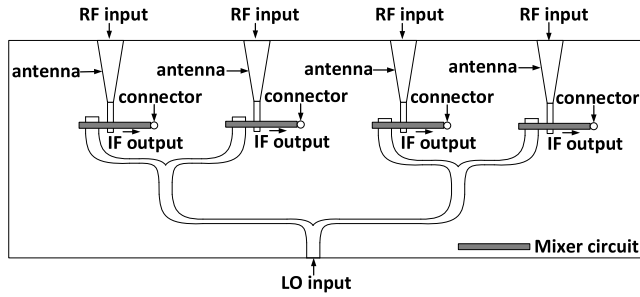


**FIGURE 1.** Configuration of the receiving front-end in the 220 GHz imaging system.

China’s ongoing project of the 220 GHz focal plane array passive imaging system is shown in Fig. 1. The consistent performances of each channel are also required, which bring challenges to the submillimeter wave and THz mixers.

Mixer as the key component of the submillimeter wave receiver directly determines the receiver’s performances especially when there is no proper wideband THz LNA in the system. In the past few decades, the application of planar Schottky diodes greatly contributes to the development of the submillimeter wave and terahertz mixers operating at room temperature. In the previous researches, mixers based on Schottky diodes exhibit good performances with frequency up to 2.5 THz [9], [10]. Discrete diodes or flip chip diodes are preferred to realize mixers at lower frequency of terahertz band for their easier approaches and good performances. However, for higher frequency circuits, the circuit designs based on flip chip diodes are limited by the thickness of the support substrates, due to increasing parasitics and the generation of higher modes. Meanwhile, as the operating frequency wavelength of the discrete Schottky diodes moves in to submillimeter wave and terahertz range, the performances of mixers and consistency of the performances are challenged due to the fabricating process, which would not meet the demand of imaging arrays.

GaAs MMIC (millimeter-wave monolithic integrated circuit) membrane Schottky diode is an ideal option to solve these problems by integrating the diodes on the GaAs membranes. This integration technology can reduce the parasitic elements compared with flip chip diodes. It can simplify the fabrication and realize stable and consistent performances of the mixer. Another significant advantage of GaAs integrated Schottky diodes is that, the geometry and dimensions of the integrated diodes can be optimized according to their specific applications, thus the performances of the circuits can be improved. This advantage is especially important at higher frequency of THz band. With GaAs monolithic integration technology, it’s potential to supply a large number of identical high frequency circuits based on GaAs Schottky diodes without the effort of developing complicated fabrication technology. This could benefit the researches and development of large-scale imaging array by improving the consistency of each receiving channel and reducing the

expense of fabrication. In the past few years, a number of mixers based on GaAs monolithic integration technology have been developed and exhibit good performances at submillimeter wave and THz band [11]–[15].

In this paper, a 220 GHz wideband subharmonic mixer based on GaAs monolithic integration technology is proposed. The GaAs membrane Schottky diode is designed by UESTC and manufactured in Hebei Semiconductor Research Institute. 12 μm-thickness GaAs membrane is applied with anti-parallel Schottky diodes directly fabricated on it. The geometry and dimensions of the GaAs MMIC membrane Schottky diodes are optimized to reduce parasitic elements, and the fabrication process is also introduced. Based on the combination of load-pull technique and harmonic balance simulation, the matching network of the proposed mixer is obtained. To meet the requirements for both active and passive imaging systems, the wide RF and IF bandwidths of the mixer are essential. To increase the IF bandwidth which is especially important for passive imaging system, a wideband IF LPF with improved CMRC configuration and a wideband perpendicular coax-microstrip connection is applied. The proposed 220 GHz mixer exhibits wideband performances and will be applied in the 220 GHz imaging systems in the future.

## II. DEVELOPMENT OF THE GaAs MMIC MEMBRANE SCHOTTKY DIODES

GaAs monolithic integration technology has been developed to improve the performances of the mixer by integrating specialized Schottky diodes on GaAs membranes. The configuration and cross section view of the GaAs MMIC membrane diodes are shown in Fig. 2. The anode is formed on the GaAs epitaxial layer with a SiO<sub>2</sub> layer providing passivation and insulation. An ohmic contact is also deposited on one end of the chip connecting to the anode by means of a narrow finger. The bridge metals are used to connect the cathode pads of the diodes to the external matching circuits. Compared

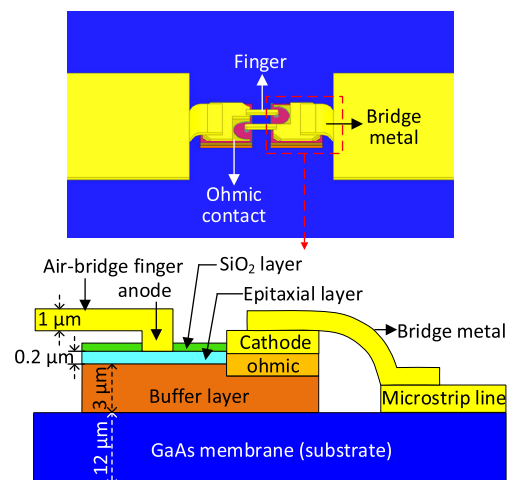


**FIGURE 2.** Configuration and cross section view of the GaAs MMIC membrane Schottky diodes.

with flip chip diodes, the MMIC technology offers substantial advantages in the production of high frequency circuits due to their ability to develop high quality, low-parasitics Schottky diodes and incorporate both Schottky structures and external matching circuits on a single substrate. In this paper, the dimensions and main parameters of the GaAs MMIC membrane diode are optimized to realize good performances of the 220 GHz harmonic mixer.

**A. OPTIMIZATION OF THE LOW-PARASITICS GaAs MMIC MEMBRANE DIODES**

The performances of planar GaAs Schottky diodes degrade at THz region as a result of the high frequency parasitic effects. These parasitic elements of Schottky diodes are complex and distributed. Main parasitic elements of the Schottky diode are shown in Fig. 3, including resistances, inductances and capacitances. The parasitic resistance consists of four parts: the epitaxial layer resistance  $R_{epi}$ , the buffer region resistance  $R_{buffer}$ , the ohmic contact resistance  $R_{ohmic}$ , and the air bridge resistance  $R_{finger}$ . Among these resistances,  $R_{epi}$  is the dominant part. The parasitic capacitance is comprised of two main parts: finger capacitance ( $C_f$ ) and pad capacitance ( $C_p$ ).  $C_{p1}$  and  $C_{p2}$  represent electrical coupling between contact pads through air and semi-insulating GaAs substrate, respectively. All these parasitic parameters contribute to the degradation of the diode performances. The geometry and main parameters of the Schottky diodes are optimized with following steps to reduce parasitic elements of the diodes.

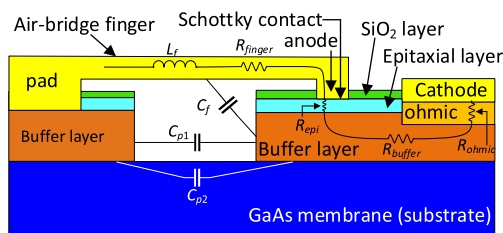


**FIGURE 3. Parasitic elements of typical planar Schottky diode [16]–[21].**

a) Choosing high doping density for the epitaxial layer. Several researches [16], [17] have been done, revealing that increasing the doping density will mitigate the hot-electron noise, which plays an important role in the noise of diode at terahertz band. Apart from that, improving the doping density of the epitaxial layer is essential to reduce the series resistance of the diode. In this paper, the doping density of  $5 \times 10^{17} \text{ cm}^{-3}$  is applied. A thin epitaxial layer is preferred for low series resistance. The thickness of this layer of the proposed GaAs MMIC membrane diode is 200 nm in this paper.

b) Reducing the parasitic capacitances by optimizing the shape of the diode. Parasitic capacitances limit the cutoff frequency and bandwidth of any mixer. Capacitance between the contact pads is normally the largest shunt capacitance. Lots of researches have been done to reduce parasitic capacitances of Schottky diodes [18]–[21]. Large scale models and numerical analyses indicate that pad capacitance is reduced

by reducing pad area, increasing pad separation, decreasing substrate dielectric constant and substrate thickness, increasing the depth of the trench, and producing trench sidewalls which have vertical or retrograde slope. The geometry and main parameters of the Schottky diodes are therefore optimized with following steps to realize good performances of the mixer.

Firstly, an effective solution to decrease pad-to-pad capacitance ( $C_{p2}$ ) is reducing the substrate thickness, especially for GaAs substrate with high dielectric constant. Due to the inherent brittleness of GaAs wafers, extreme thin membrane will bring difficulty to handling during the substrate fabrication. Therefore, a thickness of 12  $\mu\text{m}$  is chosen for the GaAs membrane in this design.

Secondly, the pad-to-pad capacitance ( $C_{p1}$ ) could be decreased by etching deep trench on the substrate of the Schottky diode. Meanwhile, the shape of the surface channel due to different surface-channel formation methods (either wet or dry etching method) also influences the parasitic capacitance of the diode. In this design, etching deep trench is impractical due to the thin GaAs membrane on which the diodes are integrated. With the methods introduced in [17], the parasitic capacitances based on the straight isolation walls and slanted isolation walls (45° angle between the membrane substrate and the slanted side wall is assumed) shown in Fig. 4 are calculated. The calculated parasitic capacitances shown in Table 1 show the straight isolation walls lead to lower pad capacitance and finger capacitance compared with slanted isolation walls. Therefore, the straight isolation walls of the Schottky diode are applied in this design.

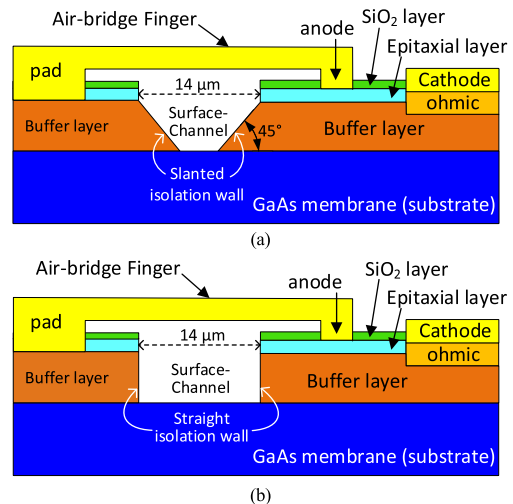


**FIGURE 4. Cross section views of the planar Schottky diode with (a) slanted and (b) straight isolation walls [21].**

Apart from that, the size of the pad area could be reduced to decrease the parasitic capacitance. For flip chip diodes, pad dimensions are limited by the process of handling and bonding in which small dimensions can make fabrication process tough and unrepeatable. The GaAs MMIC membrane Schottky diodes can overcome this problem by connecting

**TABLE 1. Parasitic capacitances for various etch profiles.**

Etch profile	Pad capacitances		Finger capacitances	
	$C_p$ (fF)		$C_f$ (fF)	
Straight	1.15		1.32	
Slanted (45°)	1.46		1.57	

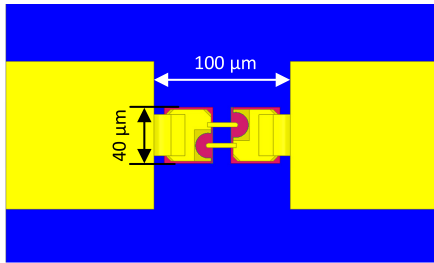


**FIGURE 5. Dimensions of the anti-parallel integrated Schottky diodes.**

the pad to the circuits with bridge metals, thus the pad dimensions can be controlled. In this design, the relatively small pad dimensions are applied. As shown in Fig. 5, the planar dimensions of the anti-parallel Schottky diodes are  $100 \mu\text{m} \times 40 \mu\text{m}$ .

c) Optimizing the anode size. Based on the doping density and other parameters of the diode, the anode size is optimized to realize good performances including low conversion loss and low optimal LO power. Reducing the size of the anode will lead to the decrease of the junction capacitance but will also increase the series resistance. The optimizing process is detailed in the part B of Section III, the simulation of the ideal mixers is carried out with harmonic balance simulation in ADS. Based on the simulation, the anode diameter of the diode to realize best performances can be obtained.

**B. FABRICATION OF THE GaAs MMIC MEMBRANE DIODES**

With the aforementioned optimized structures, the integrated Schottky diodes are fabricated with the following steps.

a) Deposition, patterning and etching of passivation layer. The starting material is a semi-insulating GaAs substrate with the epitaxial and buffer layers grown on it by MOCVD (metal-organic chemical vapor deposition), shown in Fig. 6(a). The surface of the epitaxial layer is passivated by depositing a thin film of  $\text{SiO}_2$ . Then this  $\text{SiO}_2$  layer is etched as shown in Fig. 6(b).

b) Etching of the epitaxial layer, highly-doped buffer layer and formation of the ohmic contact. This process is shown in Fig. 6(c). The thicknesses of the epitaxial layer and the buffer layer are 200 nm and  $3 \mu\text{m}$  respectively. Circular anode wells are etched by standard lithography and reactive ion etching [22]. The ohmic contact is an alloyed Au/Ge/Ni/Ag metallization, recessed into the highly-doped buffer layer.

c) Formation of the finger, cathode pad and bridge metal. The cathode pad is formed on the ohmic contact. As shown in Fig. 6(d), an air-bridge process is used to define the anode,

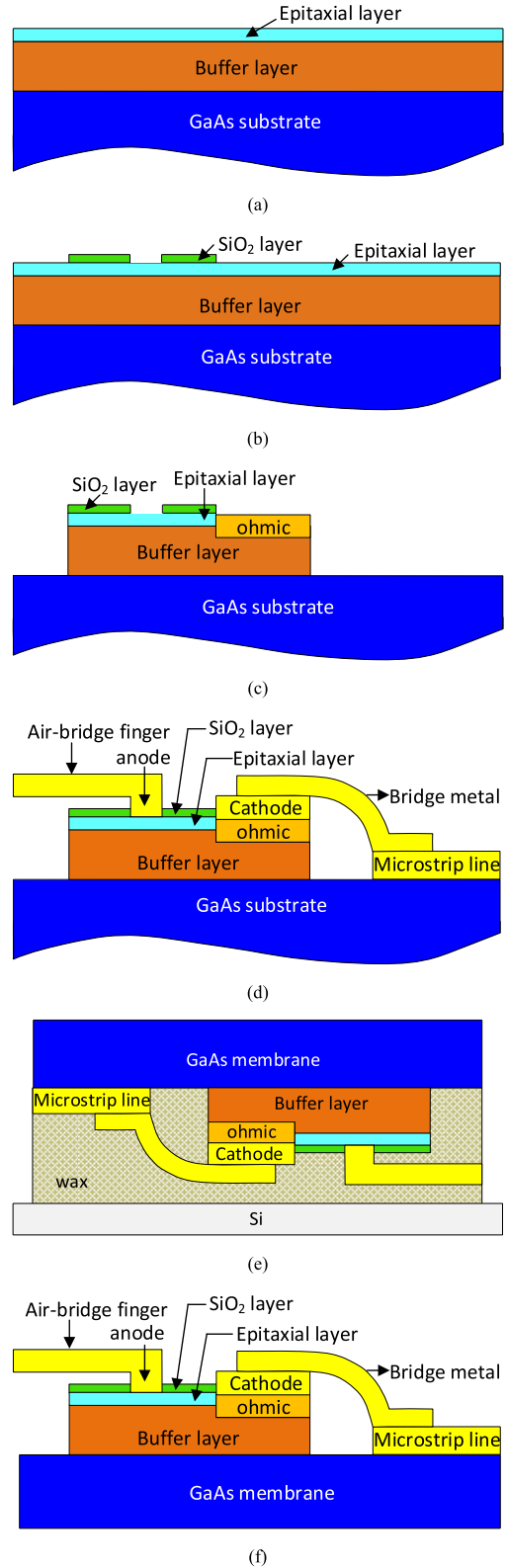


**FIGURE 6. Fabrication process of the GaAs MMIC membrane Schottky diodes.**

airbridge finger and the bridge metal which connects the transmission line of the external matching network in the same process step.

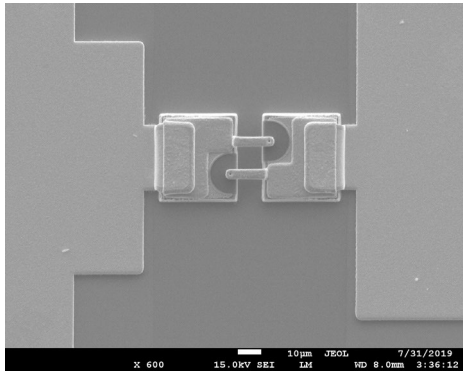


**FIGURE 7.** SEM photograph of the proposed GaAs MMIC membrane Schottky diode proposed in this paper.

d) Thinning the GaAs substrate from backside. The wafer is then mounted upside-down onto a silicon carrier wafer using wax, shown in Fig. 6(e). The GaAs substrate is thinned to the desired thickness ( $12 \mu\text{m}$ ) by lapping, polishing and wet etching. Finally, the integrated diodes are removed from the carrier wafer by dissolving the mounting wax and the integrated Schottky diodes based on GaAs membrane are obtained, shown in Fig. 6(f).

The GaAs MMIC membrane Schottky diodes with optimized structures and dimensions were fabricated with the aforementioned process in Hebei Semiconductor Research Institute. The integral dimensions of the integrated Schottky diodes (including the bridge metals) on the GaAs membrane are  $100 \mu\text{m} \times 40 \mu\text{m} \times 8 \mu\text{m}$ . Scanning electron microscope (SEM) photograph of the GaAs MMIC membrane Schottky diodes is shown in Fig. 7.

### III. CIRCUIT DESIGN

#### A. CONFIGURATION OF THE 220 GHz SUBHARMONIC MIXER BASED ON GaAs MMIC MEMBRANE SCHOTTKY DIODES

The configuration of the proposed 220 GHz subharmonic mixer based on GaAs integrated Schottky diode is shown in Fig. 8. The integral dimensions of the GaAs membrane ( $\epsilon_r = 12.9$ ) are  $4.7 \text{ mm} \times 0.42 \text{ mm} \times 0.012 \text{ mm}$ . It's suspended in an enclosed channel (with overall height of  $0.24 \text{ mm}$ ) crossing the RF and LO waveguides, which are WR8 ( $2.032 \text{ mm} \times 1.016 \text{ mm}$ ) and WR4.3 ( $1.092 \text{ mm} \times 0.546 \text{ mm}$ ) respectively. One end of the circuit is directly connected to the mechanical block providing grounding, while the other end of the circuit is soldered to the microstrip line based on Rogers 5880 substrate to output the IF signal. A GaAs membrane with a thickness of  $12 \mu\text{m}$  and dielectric constant of 12.9 is applied with Schottky diode directly manufactured on the substrate. The dimensions and parameters of the mixer diodes are optimized to realize good performances of the mixer.

To achieve the wideband mixer, the LO and RF waveguide-to-microstrip transitions are optimized using wide E-probes and waveguides with reduced height. The

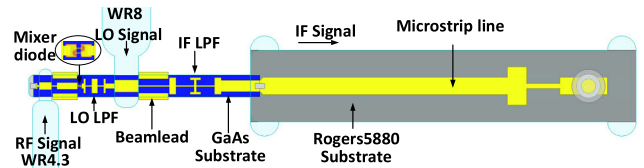


**FIGURE 8.** Configuration of the 220 GHz subharmonic mixer based on GaAs MMIC membrane Schottky diodes.

suspended microstrip is applied in the mixer for its higher Q value and less transition loss compared with microstrip structure. The dimensions of the suspended microstrip line are optimized in HFSS to ensure that the RF and LO signals are propagated on the quasi-TEM mode, and no unwanted transmission mode coupling occurs. Gold beamleads are essential to suspend the membrane in the enclosed channel. Positions of these beamleads are chosen near the RF and LO waveguides, where the impact of the mounting has the most influences. The matching networks are important for the integral performance of the mixer. Previous published literatures about wideband submillimeter wave and terahertz mixers mainly emphasize the RF bandwidth of the mixer with fixed low IF. However, for radiometers and passive imaging systems, the mixers are performed with fixed LO frequencies while the absolute RF bandwidths decide the integral performances of the systems. Therefore, the IF bandwidth needs to be broadened to guarantee wide absolute RF bandwidth. In this paper, the optimum embedding impedance of IF signal is firstly simulated with ideal nonlinear simulation. The IF low pass filter is optimized while an improved perpendicular coax-microstrip connection is applied to realize wide IF band.

#### B. OPTIMAZTION OF THE 220 GHz SUBHARMONIC MIXER

The application of the GaAs monolithic integration technology offers significant advantages by optimizing the diode's geometrical and electrical parameters to realize the best performances of the circuits. Therefore, the geometry and dimensions of the integrated diodes are firstly optimized and determined. Then the matching networks are optimized to minimize the conversion loss and noise temperature of the mixer using load-pull technique. With the combination of 3D electrical magnetic simulation in ANSYS's HFSS and harmonic balance simulation in Keysight's ADS, the simulated integral performances can be obtained.

##### 1) OPTIMIZATION OF THE INTEGRATED SCHOTTKY DIODE

The optimization principles of the Schottky diode with low parasitic elements are introduced in the previous parts, and the geometry of the integrated Schottky diode is determined. To realize best performances of the mixer, optimum size of anode, which decides the zero voltage junction capacitance of the diodes, should be chosen. Therefore, the nonlinear circuit simulation based a pair of anti-parallel ideal Schottky diodes is established in ADS to determine the zero voltage

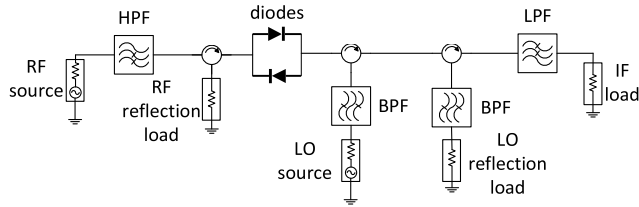


FIGURE 9. Simulation bench of the ideal mixer.

junction capacitance of the diodes for best mixer conversion loss, low RF and LO input return losses, and low LO pump power. The diagram of this simulation bench is shown in Fig. 9, ideal Schottky diodes without considering their packages and ideal filters are used in this simulation. A set of zero voltage junction capacitances (1 fF, 1.5 fF, 2 fF, 3 fF) with their corresponding series resistances of the diodes are simulated and compared. The RF signal is swept between 200 - 240 GHz, while the IF signal is fixed at 1 GHz. By tuning the embedding impedances and LO pump power, the simulated single sideband (SSB) performances and the corresponding optimum LO pump power are obtained and shown in Fig. 10. The simulation results show that with the increase of the zero voltage junction capacitance, the LO power increases. In this optimizing process, it's found that the optimum embedding impedances of the RF signal and LO signals are also influenced by the zero voltage junction capacitance of the diode. The optimum embedding impedances should be considered to realize simple matching network. Based on the analyses above, an optimum value around 1.5 fF is chosen to realize the best performance of the mixer. According to the analysis above, the anode diameter is set to be 0.8  $\mu\text{m}$  with corresponding calculated zero voltage junction capacitance of 1.4 fF.

The GaAs MMIC membrane Schottky diodes were fabricated with the aforementioned process. Main parameters of the Schottky diodes are extracted with on-wafer tested I-V and C-V characteristics of the GaAs MMIC membrane Schottky diodes. The main parameters are: saturation current,  $I_{sat} = 20$  fA, series resistance,  $R_s = 12 \Omega$ , ideality factor,  $n = 1.25$ , zero voltage junction capacitance,  $C_{j0} = 1.4$  fF.

## 2) OPTIMIZATION FOR WIDE IF BANDWIDTH

The 220 GHz subharmonic mixer applied for high sensitivity passive imaging array requires wide IF band. To realize this goal, the optimum embedding impedance of IF signal are firstly selected (80  $\Omega$  in this design) with ideal nonlinear simulation in ADS. Meanwhile, the IF low pass filter and IF perpendicular coax-microstrip connection are also optimized for wideband operation.

The IF low pass filter (LPF) of the mixer is used to isolate LO signal (operated within 90 - 130 GHz for the proposed mixer) and IF signal. To broaden the IF bandwidth, the IF LPF needs wide passband while guaranteeing high rejection at the LO band of the mixer. Compared with the traditional step-impedance filter, the improved CMRC structure

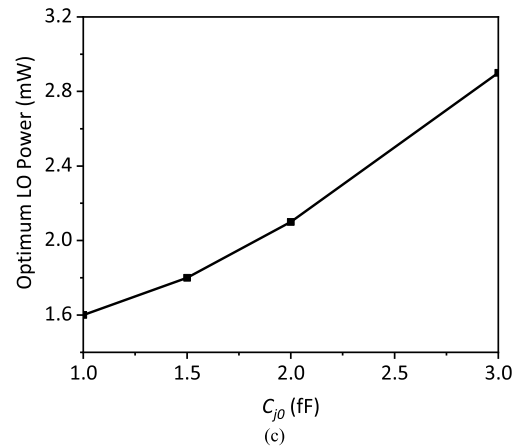
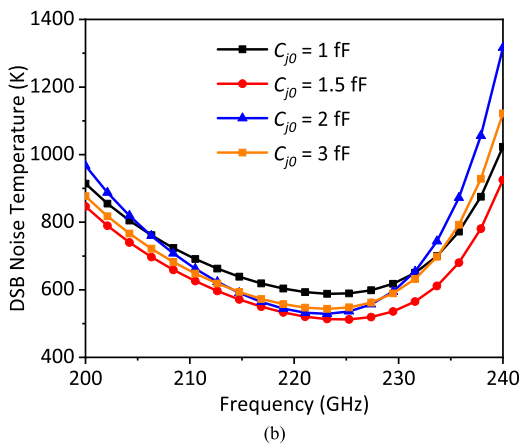
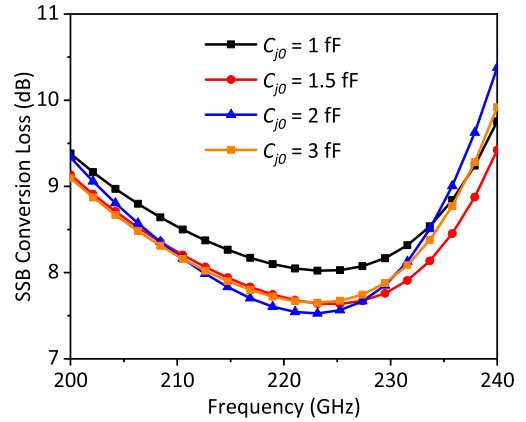
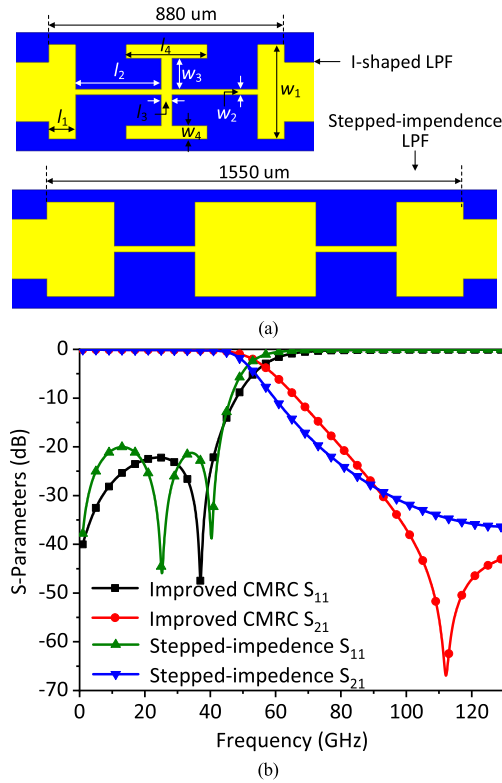


FIGURE 10. Simulated results of the ideal mixer with different zero voltage junction capacitances ( $C_{j0}$ ).

possesses good lowpass filter characteristics [23]. In this design, a improved CMRC LPF is applied to achieve this goal. As shown in Fig. 11, the proposed improved CMRC LPF is compared with a traditional stepped-impedance LPF with similar pass band and rejection band. The dimensions of this improved CMRC LPF shown in Fig. 11(a) are listed as follows:  $l_1 = 100 \mu\text{m}$ ,  $l_2 = 320 \mu\text{m}$ ,  $l_3 = 40 \mu\text{m}$ ,  $l_4 = 300 \mu\text{m}$ ,  $w_1 = 350 \mu\text{m}$ ,  $w_2 = 20 \mu\text{m}$ ,  $w_3 = 115 \mu\text{m}$ ,  $w_4 = 50 \mu\text{m}$ .



**FIGURE 11. Configuration and simulated results of the IF low pass filter: (a) the proposed improved CMRC LPF and stepped-impedances LPF, (b) Simulated S-parameters of the improved CMRC LPF and stepped-impedance LPF.**

According to the simulated S-parameters in Fig. 11(b), the improved CMRC LPF achieves low insertion loss ( $<0.2$  dB) within the passband from DC to 40 GHz and high rejection ( $>30$  dB) from 90 to 130 GHz. Compared with the stepped impedance LPF, the improved CMRC LPF features much shorter length and higher rejection within 90 - 130 GHz. The proposed improved CMRC LPF realizes wide passband and high rejection at stopband with compact size, which can meet the demand of wideband IF LPF. It's further optimized with the LO waveguide-stripline transition, and the wideband IF circuit can be obtained.

Meanwhile, a wideband coax-microstrip connection is needed to guarantee wide IF band of the mixer. For the proposed mixer designed with thin GaAs membrane, the whole circuit is flipped and suspended in an enclosed channel, thus the pin of the coax connector can't be directly connected to the GaAs substrate. Therefore, the IF output of the GaAs substrate is soldered to the microstrip transmission line on Rogers 5880 substrate with silver epoxy, while a 2.92 mm connector (with operating frequency up to 40 GHz) is then connected to the microstrip line to realize IF output. For receiving arrays with multiple channels and mixers integrated in one block (such as the one shown in Fig. 1), perpendicular coax-microstrip connections are essential for compact configurations.

In several previous researches, the output of the IF circuits is connected to the pin of the connector with bondwires [22].

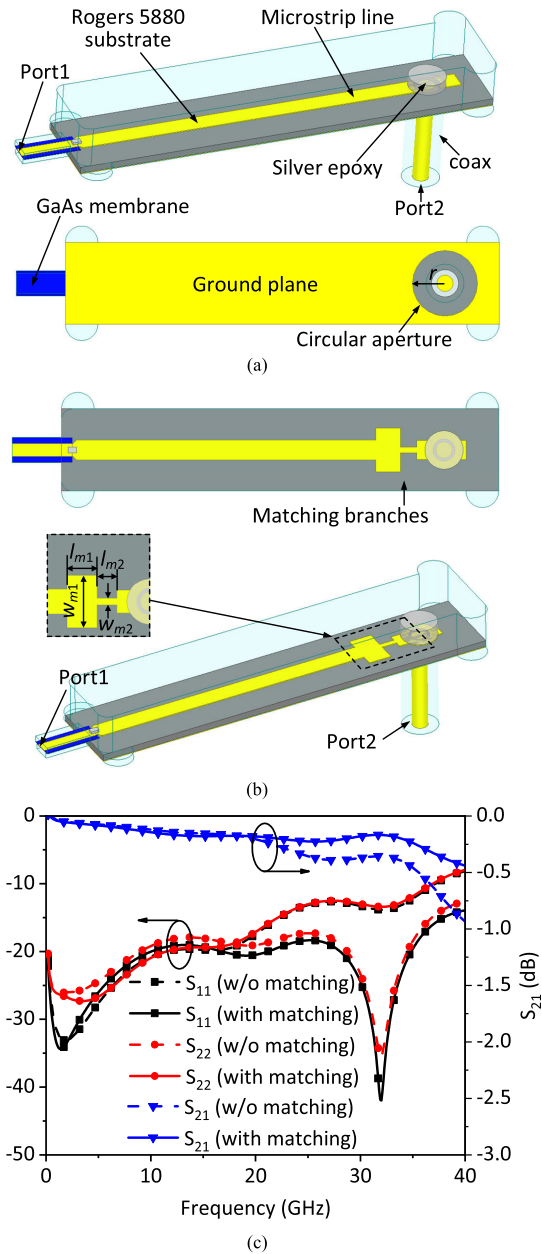


**FIGURE 12. Structures of the IF perpendicular coax-microstrip connection and the simulated results: (a) connection without matching branches, (b) connection with matching branches, (c) simulation results.**

However, thin pins of high frequency connector (diameter of 0.3 mm for the applied 2.92 mm connector) make this structure fragile. In this paper, a robust connection is proposed. The structure of the perpendicular coax-microstrip connection is shown in Fig. 12(a). The output part of GaAs membrane is mounted on the Rogers 5880 substrate and connected to the microstrip line with silver epoxy. The pin of the 2.92 mm connector penetrates through the substrate and it's welded to the annular pad on the Rogers 5880 substrate. The optimized radius of the circular aperture on the ground plane is  $r = 600 \mu\text{m}$ . This robust connection is further

optimized with stepped-impedance matching branches as shown in Fig. 12(b). The dimensions of the matching branches are listed as follows:  $l_{m1} = 450 \mu\text{m}$ ,  $l_{m2} = 400 \mu\text{m}$ ,  $w_{m1} = 800 \mu\text{m}$ ,  $w_{m2} = 350 \mu\text{m}$ . Simulated results in Fig. 12(c) show that this optimized structure exhibits good performance from DC to 40 GHz.

### 3) MATCHING NETWORK OPTIMIZATION

Based on the 3D model and electrical parameters of the proposed low-parasitics integrated Schottky diodes, the optimum embedding impedances of the RF, LO and IF signals are obtained. Then the matching network of the subharmonic mixer can be developed with 3D EM simulation and harmonic balance simulation.

The diagram of the optimizing techniques based on load-pull simulation is shown in Fig. 13. The diode model with combination of 3D model and nonlinear model of the diodes are used in this process. To validate the mixer's wideband characteristics, the simulations are respectively carried out with fixed IF frequency of 1 GHz and fixed LO frequency of 110 GHz. The simulated results show that the IF load impedance influences the IF bandwidth and conversion loss of the mixer. With a set of iterations in ADS, the optimum embedding impedances are obtained. The best performances are realized with optimum RF embedding impedance  $Z_{RF} = (40 + j79) \Omega$  at 220 GHz and optimum LO embedding impedance  $Z_{LO} = (86 + j128) \Omega$  at 110 GHz, while the optimized IF load impedance is  $80 \Omega$ .

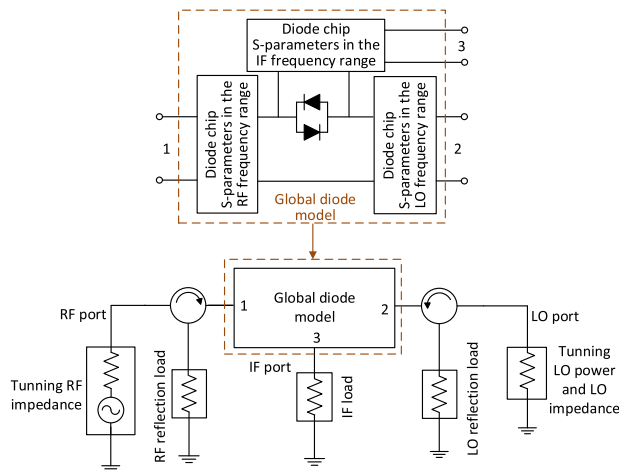
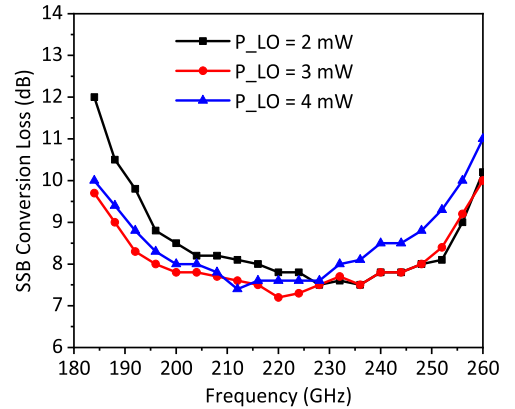
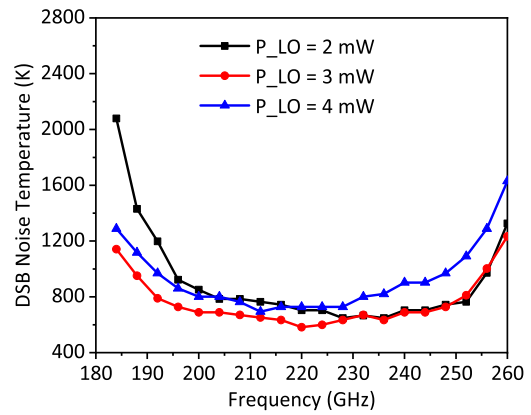


FIGURE 13. Simulation of the mixer based on load-pull technique.

For wideband operation of the mixer, the RF and LO waveguide-to-stripline transitions, low-pass filters are optimized in HFSS. Each part of the mixer circuit is simulated separately using HFSS and exported as S-parameter Touchstone file into ADS. In this process, the integrated Schottky diodes are simulated from the stripline connected by bridge metal to the diode ports. An integration line between the outer and inner conductors of the diode port is used to set the right polarity of the diodes in the integral circuit simulations.



(a)



(b)

FIGURE 14. Simulated performances of the proposed mixer with fixed IF frequency (1 GHz): (a) SSB conversion loss, (b) DSB noise temperature.

Using the nonlinear simulation software ADS, the matching network are developed and optimized.

### C. SIMULATED PERFORMANCES OF THE 220 GHz SUBHARMONIC MIXER

With the aforementioned optimizing process, the simulated performances of the mixer including conversion loss and noise temperature are carried out with harmonic balance simulation in ADS. The conversion losses of the mixer are simulated with fixed IF frequency of 1 GHz and fixed LO frequency of 110 GHz. As for the calculation of noise temperature, the standard ADS model includes thermal and shot noise sources. However, it does not include sources for hot electron noise, which has huge impact at submillimeter-wave frequencies for small anode devices. Therefore, an additional noise source is added into the diode model representing the hot electron noise to simulate the mixer based on Schottky diodes more accurately. The simulation method is introduced in [15] in detail. The noise temperature of the mixer is simulated with fixed low IF frequency (300 MHz in this paper, corresponding with the measurement), and the noise temperature at each RF frequency is obtained by tuning the frequency and pumped power of the LO signal.



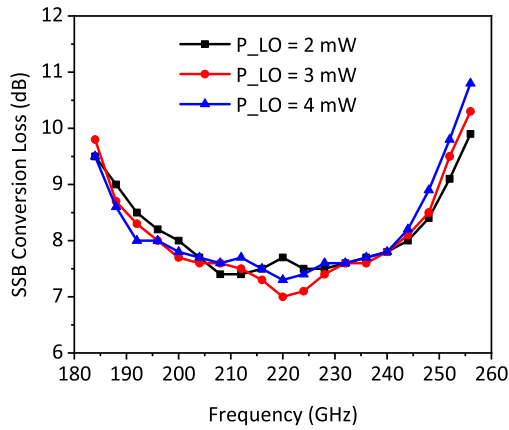


FIGURE 15. Simulated performances of the proposed mixer with fixed LO frequency of 110 GHz.

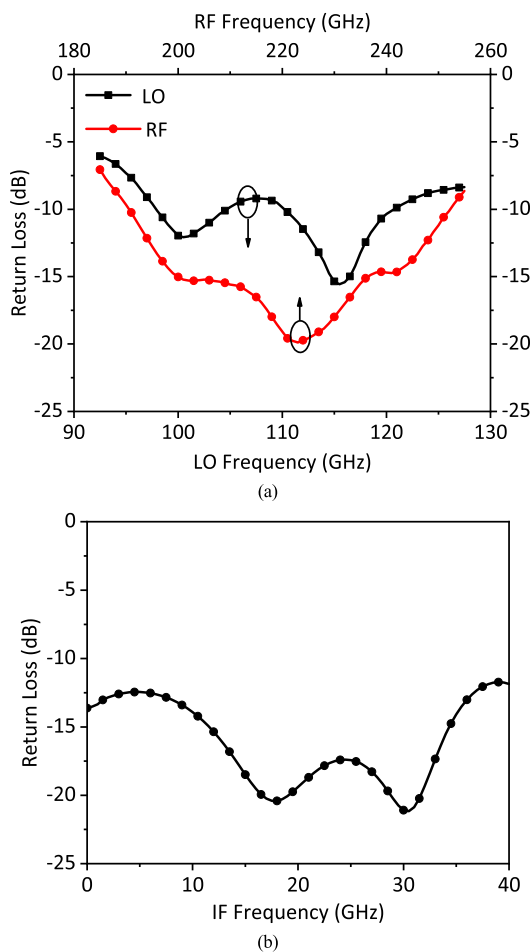


FIGURE 16. Simulated return loss of (a) RF and LO ports, (b) IF port.

The simulated performances of the 220 GHz subharmonic mixer with 1 GHz IF frequency are shown in Fig. 14. The SSB conversion loss is 7 - 10 dB from 185 to 255 GHz, while the double sideband (DSB) noise temperature is 580 - 1100 K within this frequency band. According to the performances with different LO power, an optimum LO power

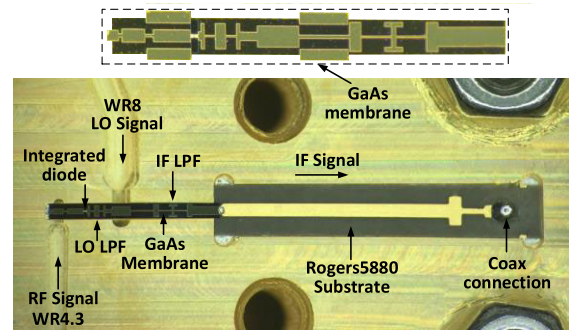


FIGURE 17. Photograph of the proposed mixer circuit mounted on the half of the split metal block.

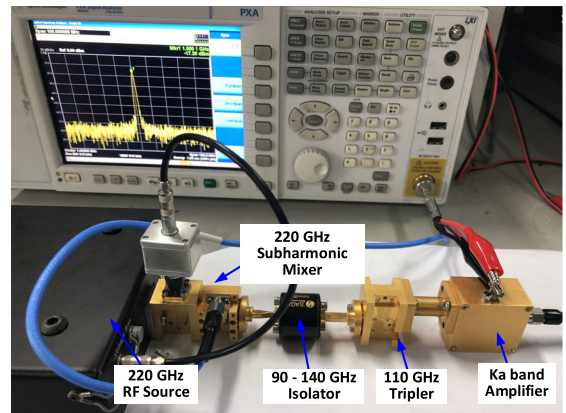


FIGURE 18. Photograph of the test setup for the SSB conversion loss of the 220 GHz mixer.

level of 3 mW is obtained. Meanwhile, the mixer’s simulated performances with fixed LO frequency of 110 GHz are shown in Fig. 15. The SSB conversion loss is below 11 dB from 185 to 255 GHz with LO power level of 3 mW. It shows that the proposed mixer can cover the RF band of 185 - 255 GHz and IF band of DC - 35 GHz.

Meanwhile, the return loss of each port is simulated in Keysight’s ADS and shown in Fig. 16. The return loss of the RF port is better than 10 dB from 190 to 250 GHz, while the return loss of the LO port is better than 9 dB from 97 to 123 GHz. As for the IF port, the return loss is simulated with fixed LO frequency of 110 GHz. The simulated results in Fig. 16 (b) indicate the wide IF band of the proposed mixer.

#### IV. MEASUREMENT AND COMPARISON

Based on the aforementioned optimization techniques and simulations, the GaAs membranes with Schottky diodes integrated on it were manufactured in Hebei Semiconductor Research Institute while the 220 GHz subharmonic mixers were fabricated and measured in UESTC. Photograph of the proposed circuits mounted on the lower half of the split metal block is shown in Fig. 17. The GaAs membrane is supported in the air channel with gold beamleads. Meanwhile, the IF output port of the GaAs circuits is connected to a Rogers 5880 substrate and the IF signal is output with the wideband

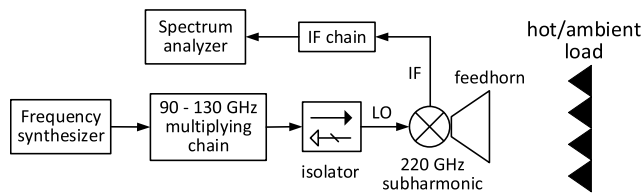


FIGURE 19. Diagram of the noise temperature measuring platform based on the Y factor.

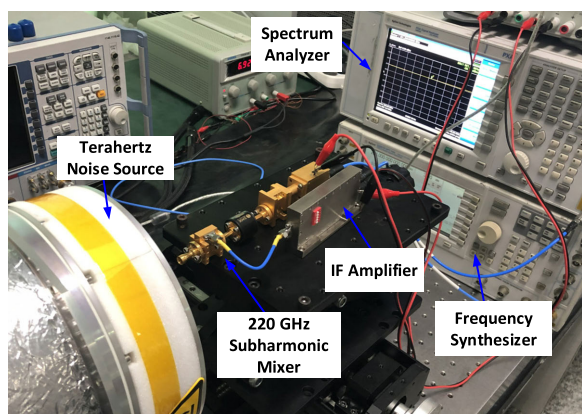


FIGURE 20. Photograph of the measuring platform for the DSB noise temperature of the 220 GHz mixer.

perpendicular coax-microstrip connection. All measurements of the 220 GHz subharmonic mixer are performed at room temperature. In the measurement of conversion loss, a  $\times 3$  multiplier chain and signal generator (E8267D from Agilent) is used to supply sufficient LO power for the mixer within the operating frequency range from 90 to 130 GHz. To reduce the influence of the LO sources, such as the potential power reflection at the mixer’s LO port, the STF-08-S1 isolator (from Sage Millimeter Inc.) with insertion loss of 2.0 dB and isolation of 30 dB is applied. A  $\times 18$  multiplier chain is used to provide RF signal, which is calibrated by THz power meter (Erickson’s PM4), while the IF signal is measured with spectrum analyzer (Agilent’s N9030A). Photograph of the test platform is shown in Fig. 18. The LO pump power of the mixer is tuned to achieve the best performances during the experiment.

As for the measurement of the noise temperature, the Y factor method and gain procedure introduced in [24] is applied to obtain the noise temperature of the mixer. The Y factor measurements are performed by presenting hot and cold blackbody loads to the feedhorn input. In Fig. 19, the diagram of the measuring platform based on the Y factor method is illustrated. As shown in Fig. 20, the hot and ambient calibration loads (from TK Inc.) are used as calibrated noise sources. A narrowband IF amplifier with operating frequency of 240 - 360 MHz and tunable gain is applied while its output is measured by the spectrum analyzer. The LO pump power of the mixer is tuned to achieve the best performances during the experiment.

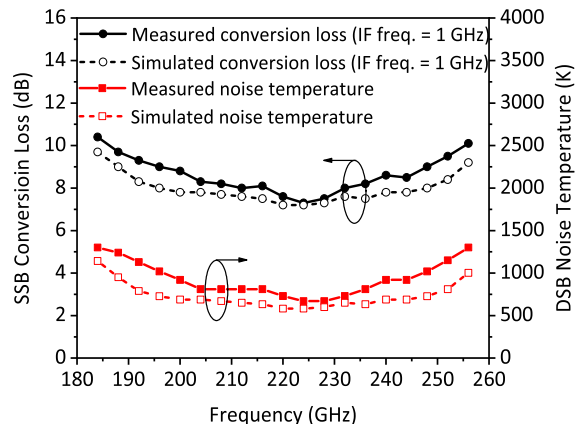


FIGURE 21. Comparison between the simulated and measured performances of the 220 GHz mixer with fixed IF frequency.

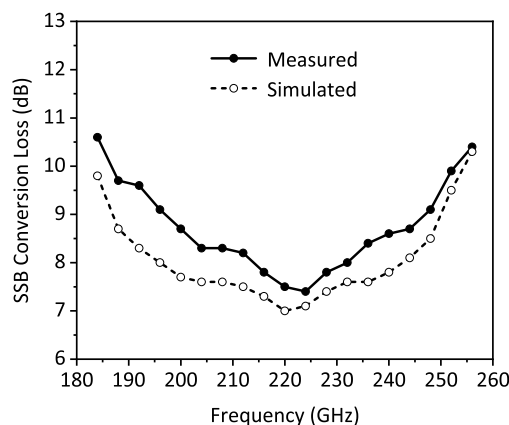


FIGURE 22. Comparison between the simulated and measured performance of the 220 GHz mixer with fixed LO frequency of 110 GHz.

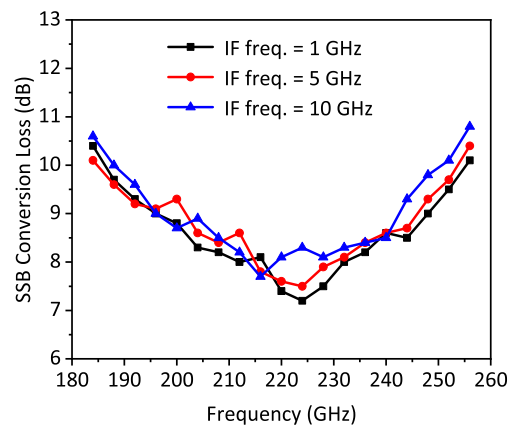


FIGURE 23. Measured conversion loss of the mixer with different IF frequency (IF = 1 GHz, IF = 5 GHz, IF = 10 GHz).

In Fig. 21, the measured performances of the mixer with fixed IF frequency are presented together with the simulated results. Good agreement between the measured and simulated results is achieved. The measured DSB noise temperature and SSB conversion loss are below 1400 K and 10.5 dB

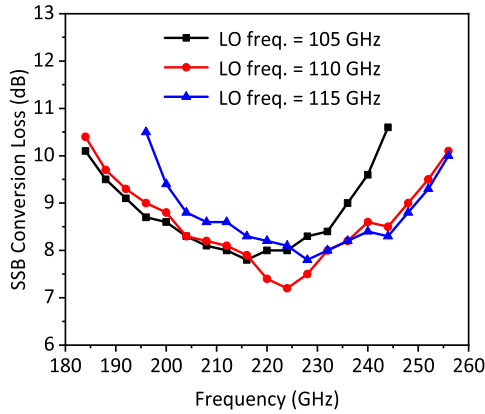


FIGURE 24. Measured conversion loss of the mixer with different LO frequency (LO freq. = 105 GHz, LO freq. = 110 GHz, LO freq. = 115 GHz).

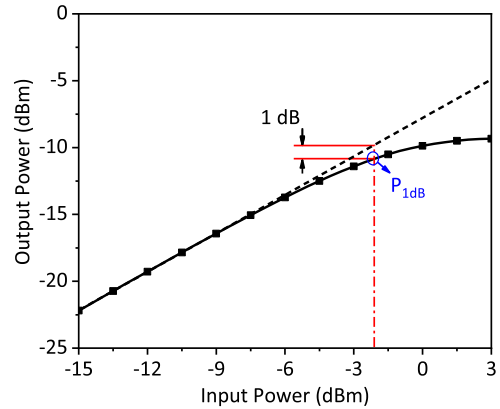


FIGURE 26. Measured IF output power with different RF input power when the LO frequency is 110 GHz and the IF frequency is 1 GHz.

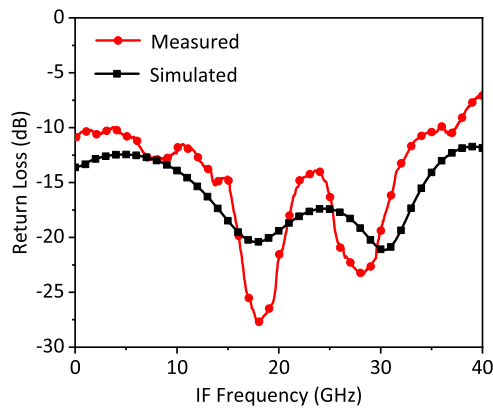


FIGURE 25. Simulated and measured return loss of the IF port of the mixer.

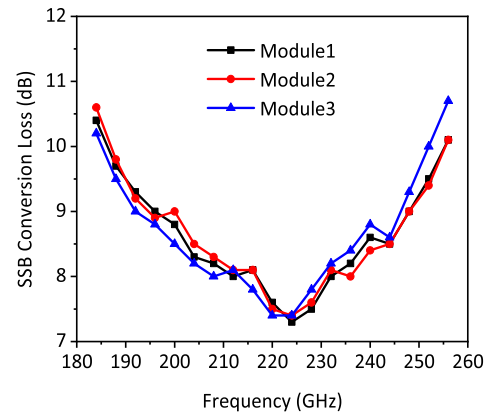


FIGURE 27. Comparison between the measured performances (IF freq. = 1 GHz) of three 220 GHz mixers using GaAs circuits manufactured in one batch.

respectively over the frequency range of 185 – 255 GHz. The optimum LO power obtained in the measurement is 3 mW. The best performances are achieved at 224 GHz with lowest DSB noise temperature of 670 K and lowest SSB conversion loss of 7.2 dB.

The mixer was also measured with fixed LO frequency of 110 GHz. The measured results in Fig. 22 show that the SSB conversion loss within 185 - 255 GHz is 7.4 - 10.7 dB with optimum LO power of 3 mW, which also agree well with the simulated results. It shows the proposed mixer’s good performances with IF frequency from DC to 35 GHz. The differences between the measured and simulated results are brought by inaccurately modeling of diodes and mixer circuits. The slight differences between the designed diodes and manufactured ones may also lead to the differences between the measured and simulated results.

The proposed 220 GHz subharmonic mixer is also measured with different IF frequencies and LO frequencies. Measured results in Fig. 23 and Fig. 24 exhibit the wideband performances of the mixer.

To validate the wide IF band of the mixer, the return loss of IF port is measured with vector network analyzer (Agilent’s

N5244A). Measured results in Fig. 25 show that the IF return loss is better than 10 dB from 0.1 to 35 GHz.

The linearity of the proposed 220 GHz mixer is also measured with fixed LO frequency of 110 GHz and IF frequency of 1 GHz. The relation between the input RF power and output IF power is shown in Fig. 26. It shows that the  $P_{1dB}$  of the mixer is about  $-2$  dBm.

Meanwhile, the consistency of the performances of the proposed 220 GHz mixer based on GaAs monolithic integration technology is examined by comparing the conversion loss of three modules fabricated with same GaAs circuits manufactured in one batch. The measured results in Fig. 27 validate the highly consistent performances of these modules with the technology of the integrated Schottky diodes.

Table 2 summaries the comparison between the performances of published subharmonic mixers in the similar frequency range [25]–[29]. The DSB noise temperature and the conversion loss are theoretically half of the SSB noise temperature and conversion loss. All the noise temperatures listed in Table 2 are measured with fixed and low IF frequencies, while the conversion losses are measured with either fixed LO frequency or fixed IF frequency. The comparison shows

**TABLE 2. Summary of published subharmonic mixer performance in the similar frequency range.**

Ref.	Frequency (GHz)	Noise temperature † (K)	Conversion loss ‡ (dB)	Conversion loss ‡‡ (dB)	Diode technology
[25]	210 - 250	950 - 2000	7 - 10 †	NI	Flip chip
[26]	188 - 244	680 - 1500	6.5 - 10 †	NI	Flip chip
[27]	215	3500	9.2 ††	NI	Flip chip
[28]	211 - 226	NI	8 - 11.2 ††	5.9 - 12 ††	Flip chip
[29]	198 - 238	692 - 924	NI	7.2 - 10 ††	Flip chip
<b>This work</b>	<b>185 - 255</b>	<b>670 - 1400</b>	<b>7.2 - 10.5 ††</b>	<b>7.4 - 10.7 ††</b>	<b>GaAs MMIC integrated</b>

†: DSB; ††: SSB; NI: Not Indicated; ‡: With fixed IF; ‡‡: With fixed LO of 110 GHz

the wideband performances of the proposed mixer with either fixed IF frequency or fixed LO frequency. It validates the proposed optimizing methods of both integrated diodes and mixer circuits.

The wideband characteristics enable the proposed mixer to meet the requirements of both active and passive imaging systems. Meanwhile, the technology of the integrated Schottky diodes reduces the process of fabricating the diodes and realizes highly consistent and stable performances of mixer. This provides possibility to manufacture a number of identical mixers efficiently. The proposed mixer and GaAs monolithic integration technology can be applied for the ongoing 220 GHz passive imaging array project and large-scale receiver arrays in the future.

## V. CONCLUSION

In this paper, the development of a 220 GHz wideband subharmonic mixer based on GaAs monolithic integration technology is proposed. The GaAs MMIC membrane schottky diodes are utilized to improve the performances of the mixer. The optimizing methods for low-parastics diodes and the fabrication process are introduced. Based on these methods, the geometry and dimensions of the integrated diodes are optimized while the matching networks of the mixer are realized based on load-pull technique and harmonic balance simulation. The wide RF and IF band of this mixer are achieved to meet the requirement of both active and passive imaging systems, an improved CMRC low pass filter and a wideband if perpendicular coax-microstrip connection are applied to broaden the if bandwidth. measurements show that the SSB conversion loss is 7.2 - 10.5 dB from 185 to 255 GHz with fixed RF frequency of 1 GHz, while the DSB noise temperature is 670 - 1400 K in this frequency range. With fixed LO frequency of 110 GHz, the measured SSB conversion loss is 7.4 - 11.7 dB within 185 - 255 GHz, revealing the good performances of the mixer with high RF up to 35 GHz. The 220 GHz mixer based on GaAs MMIC membrane diodes exhibits wideband characteristic and consistent performances. It will be applied in 220 GHz imaging systems in the future.

## REFERENCES

- [1] K. B. Cooper, R. J. Dengler, N. Llombart, T. Bryllert, G. Chattopadhyay, E. Schlecht, J. Gill, C. Lee, A. Skalare, I. Mehdi, and P. H. Siegel, "Penetrating 3-D imaging at 4- and 25-m range using a submillimeter-wave radar," *IEEE Trans. Microw. Theory Techn.*, vol. 56, no. 12, pp. 2771–2778, Dec. 2008.
- [2] E. Heinz, T. May, D. Born, G. Zieger, S. Anders, V. Zakosarenko, H.-G. Meyer, and C. Schäffel, "Passive 350 GHz Video Imaging Systems for Security Applications," *J. Infr., Millim., THz Waves*, vol. 36, no. 10, pp. 879–895, Oct. 2015.
- [3] G. Chattopadhyay, "Terahertz circuits, systems, and imaging instruments," in *Proc. 39th Int. Conf. Infr., Millim., THz Waves (IRMMW-THz)*, Sep. 2014, pp. 1–2.
- [4] R. Appleby and R. N. Anderton, "Millimeter-wave and submillimeter-wave imaging for security and surveillance," *Proc. IEEE*, vol. 95, no. 8, pp. 1683–1690, Aug. 2007.
- [5] K. B. Cooper, R. J. Dengler, N. Llombart, B. Thomas, G. Chattopadhyay, and P. H. Siegel, "THz imaging radar for standoff personnel screening," *IEEE Trans. THz Sci. Technol.*, vol. 1, no. 1, pp. 169–182, Sep. 2011.
- [6] F. Friederich, W. Von Spiegel, M. Bauer, F. Meng, M. D. Thomson, S. Boppel, and T. Löffler, "THz active imaging systems with real-time capabilities," *IEEE Trans. THz Sci. Techn.*, vol. 1, no. 1, pp. 183–200, Aug. 2011.
- [7] G. C. Trichopoulos, H. L. Mosbacker, D. Burdette, and K. Sertel, "A broadband focal plane array camera for real-time THz imaging applications," *IEEE Trans. Antennas Propag.*, vol. 61, no. 4, pp. 1733–1740, Apr. 2013.
- [8] T. Reck, J. Siles, C. Jung, J. Gill, C. Lee, G. Chattopadhyay, and K. Cooper, "Array technology for terahertz imaging," *Proc. SPIE*, vol. 8362, May 2012, Art. no. 836202.
- [9] P. H. Siegel, R. P. Smith, M. C. Graidis, and S. C. Martin, "2.5-THz GaAs monolithic membrane-diode mixer," *IEEE Trans. Microw. Theory Techn.*, vol. 47, no. 5, pp. 596–604, May 1999.
- [10] J. L. Hesler, H. Xu, T. Reck, and T. W. Crowe, "Development and testing of a 2.5 THz Schottky mixer," in *Proc. Int. Conf. Infr., Millim., THz Waves*, Houston, TX, USA, 2011, pp. 1–2.
- [11] B. Thomas, "An integrated 520–600 GHz sub-harmonic mixer and tripler combination based on GaAs MMIC membrane planar Schottky diodes," in *Proc. 35th Int. Conf. Infr., Millim., THz Waves*, Rome, Italy, 2010, pp. 1–2.
- [12] T. Waliwander, "Sub-millimeter wave 183 GHz and 366 GHz MMIC membrane sub-harmonic mixers," in *IEEE MTT-S Int. Microw. Symp. Dig.*, Baltimore, MD, USA, Jun. 2011, p. 1.
- [13] H. Zhao, V. Drakinskiy, P. Sobis, J. Hanning, T. Bryllert, A.-Y. Tang, and J. Stake, "Development of a 557 GHz GaAs monolithic membrane-diode mixer," in *Proc. Int. Conf. Indium Phosph. Rel. Mater.*, Santa Barbara, CA, Aug. 2012, pp. 102–105.
- [14] J. Treuttel, "A 520–620-GHz Schottky receiver front-end for planetary science and remote sensing with 1070 K–1500 K DSB noise temperature at room temperature," *IEEE Trans. THz Sci. Technol.*, vol. 6, no. 1, pp. 148–155, Jan. 2016.
- [15] B. Thomas, A. Maestrini, J. Gill, C. Lee, R. Lin, I. Mehdi, and P. De Maagt, "A Broadband 835–900-GHz fundamental balanced mixer based on monolithic GaAs membrane Schottky diodes," *IEEE Trans. Microw. Theory Techn.*, vol. 58, no. 7, pp. 1917–1924, Jul. 2010.
- [16] T. W. Crowe, R. J. Mattauch, H. P. Roser, W. L. Bishop, W. C. B. Peatman, and X. Liu, "GaAs Schottky diodes for THz mixing applications," *Proc. IEEE*, vol. 80, no. 11, pp. 1827–1841, Nov. 1992.
- [17] T. W. Crowe and R. J. Mattauch, "Analysis and optimization of millimeter- and submillimeter-wavelength mixer diodes," *IEEE Trans. Microw. Theory Techn.*, vol. 35, no. 2, pp. 159–168, Feb. 1987.
- [18] W. L. Bishop, T. W. Crowe, and R. J. Mattauch, "Planar GaAs Schottky diode fabrication: Progress and challenges," in *Proc. 4th Int. Space THz Tech. Symp.*, Los Angeles, CA, USA, Mar. 1993, pp. 1–15.
- [19] W. L. Bishop, E. R. Meiburg, R. J. Mattauch, T. W. Crowe, and L. Poli, "A micron-thickness, planar Schottky diode chip for terahertz applications with theoretical minimum parasitic capacitance," in *IEEE Int. Dig. Microw. Symp.*, Dallas, TX, USA, vol. 3, 1990, pp. 1305–1308.
- [20] J. A. Wells and N. J. Cronin, "Theoretical analysis of air bridging and back etching techniques on the shunt capacitance of planar subharmonic mixer diodes," *IEE Proc. H—Microw., Antennas Propag.*, vol. 140, no. 6, pp. 474–480, Dec. 1993.
- [21] A. Y. Tang and J. Stake, "Impact of eddy currents and crowding effects on high-frequency losses in planar Schottky diodes," *IEEE Trans. Electron Devices*, vol. 58, no. 10, pp. 3260–3269, Oct. 2011.

- [22] S. M. Marazita, W. L. Bishop, J. L. Hesler, K. Hui, W. E. Bowen, and T. W. Crowe, "Integrated GaAs Schottky mixers by spin-on-dielectric wafer bonding," *IEEE Trans. Electron Devices*, vol. 47, no. 6, pp. 1152–1157, Jun. 2000.
- [23] X.-F. Yang, Y. Fan, B. Zhang, and X. Xu, "A novel narrow passband millimeter filter using suspended improved compact microstrip resonant cell," *J. Electromagn. Waves Appl.*, vol. 25, nos. 11–12, pp. 1699–1707, Jan. 2011.
- [24] I. Maestrojuan, S. Rea, I. Ederra, and R. Gonzalo, "Experimental analysis of different measurement techniques for characterization of millimeter-wave mixers," *Microw. Opt. Technol. Lett.*, vol. 56, no. 6, pp. 1441–1447, Jun. 2014.
- [25] I. Maestrojuan, I. Palacios, I. Ederra, and R. Gonzalo, "USE of COC substrates for millimeter-wave devices," *Microw. Opt. Technol. Lett.*, vol. 57, no. 2, pp. 371–377, Feb. 2015.
- [26] Z. Chen, B. Zhang, Y. Fan, and Y. Yuan, "Design of a low noise 190–240 GHz subharmonic mixer based on 3D geometric modeling of Schottky diodes and CAD load-pull techniques," *IEICE Electron. Exp.*, vol. 13, no. 16, 2016, Art. no. 20160604.
- [27] V. S. Möttönen, P. Piironen, J. Zhang, A. V. Räisänen, C. I. Lin, A. Simon, and H. L. Hartnagel, "Subharmonic waveguide mixer at 215 GHz utilizing quasivertical Schottky diodes," *Microw. Opt. Technol. Lett.*, vol. 27, no. 2, pp. 93–97, 2000.
- [28] Y. Zhang, W. Zhao, Y. Wang, T. Ren, and Y. Chen, "A 220 GHz subharmonic mixer based on Schottky diodes with an accurate terahertz diode model," *Microw. Opt. Technol. Lett.*, vol. 58, no. 10, pp. 2311–2316, Oct. 2016.
- [29] J. Cui, Y. Zhang, D. Xia, Y. Xu, F. Xiao, B. Yan, and R. Xu, "A 220 GHz broadband sub-harmonic mixer based on global design method," *IEEE Access*, vol. 7, pp. 30067–30078, 2019.



**YILIN YANG** received the B.E. degree in electronic field and wireless technology from the University of Electronic Science and Technology of China, Chengdu, Sichuan, China, in 2013, where he is currently pursuing the Ph.D. degree in electromagnetic fields and microwave technology with the School of Electronic Engineering. His research interests focus on modeling of semiconductor devices at THz band, THz modules in transmitters and receivers, and THz systems for the imaging application.



**BO ZHANG** (Senior Member, IEEE) received the B.E., M.S., and Ph.D. degrees in electromagnetic field and microwave technology from the University of Electronic Science and Technology of China, Chengdu, China, in 2004, 2007, and 2011, respectively.

He is currently a Professor with the School of Electronic Science and Engineering, University of Electronic Science and Technology of China. His research interests are terahertz solid state technology and systems.



**DONGFENG JI** received the B.E. degree in electrical engineering from the University of Electronic Science and Technology of China (UESTC), Chengdu, China, in 2013, where he is currently pursuing the Ph.D. degree in electrical engineering with the School of Electronic Science and Engineering. His research interest includes the microwave and THz solid-state devices, circuits, and systems.



**XIANGYANG ZHAO** received the B.E. degree in applied physics from the University of Electronic Science and Technology of China, Chengdu, China, in 2013, and the M.S. degree in microelectronics and solid-state electronics from the China Electronics Technology Group Corporation, Academy of Electronics and Information Technology, China, in 2016.

He is currently a member of the Technical Staff with the National Key Laboratory of ASIC, Hebei Semiconductor Research Institute, Shijiazhuang, China. His research interest includes modeling and optimization of Schottky diode for terahertz application.



**YONG FAN** received the B.E. degree from the Nanjing University of Science and Technology, Jiangsu, China, in 1985, and the M.S. degree in microwave technology from the University of Electronic Science and Technology of China, Chengdu, China, in 1992.

He is currently a Professor and the Dean of the School of Electronic Science and Engineering, University of Electronic Science and Technology of China. His research interests are millimeter wave and terahertz technology and systems.



**XIAODONG CHEN** (Fellow, IEEE) received the B.Sc. degree in electronic engineering from the University of Zhejiang, Hangzhou, China, in 1983, and the Ph.D. degree in microwave electronics from the University of Electronic Science and Technology of China, Chengdu, China, in 1988.

In 1988, he joined the Department of Electronic Engineering, King's College, University of London, London, U.K., as a Postdoctoral Visiting Fellow. In 1990, he was a Research Associate with King's College, where he was appointed to an EEV Lectureship. In 1999, he joined the School of Electronic Engineering and Computer Science, Queen Mary University of London, where he is currently a Professor. His research interests are in the fields of wireless communications, microwave devices, and antennas. He has authored or coauthored many publications (book chapters, journal articles, and refereed conference presentations).

...